Biogeosciences Discuss., 8, 11899–11939, 2011
www.biogeosciences-discuss.net/8/11899/2011/
doi:10.5194/bgd-8-11899-2011
© Author(s) 2011. CC Attribution 3.0 License.

Biogeosciences Discussions

This discussion paper is/has been under review for the journal Biogeosciences (BG).
Please refer to the corresponding final paper in BG if available.

Towards a merged satellite and in situ fluorescence ocean chlorophyll product

H. Lavigne[1,2], **F. D'Ortenzio**[1,2], **H. Claustre**[1,2], **and A. Poteau**[1,2]

[1]CNRS, UMR 7093, Laboratoire d'Océanographie de Villefranche, 06230 Villefranche sur-Mer, France
[2]Université Pierre et Marie Curie-Paris 6, UMR 7093, Laboratoire d'Océanographie de Villefranche, 06230 Villefranche-sur-Mer, France

Received: 2 November 2011 – Accepted: 26 November 2011 – Published: 13 December 2011

Correspondence to: H. Lavigne (heloise.lavigne@obs-vlfr.fr)

Published by Copernicus Publications on behalf of the European Geosciences Union.

Abstract

Understanding the ocean carbon cycle requires a precise assessment of phytoplankton biomass in the oceans. In terms of numbers of observations, satellite data represents the largest available data set. However, as they are limited to surface waters, they have to be merged with in situ observations. Amongst the in situ data, fluorescence profiles constitute the greatest data set available, because fluorometers operate routinely on oceanographic cruise since the seventies. Nevertheless, fluorescence is only a proxy of the Total Chlorophyll-*a* concentration and a data calibration is required. Calibration issues are, however, source of uncertainty and they have prevented a systematic and wide range exploitation of the fluorescence data set. In particular, very few attempts to standardize the fluorescence data bases exist. Consequently, merged estimations with other data sources (i.e. satellite) are lacking.

We propose a merging method to fill this gap. It consists firstly, in adjusting the fluorescence profile to impose a zero Chlorophyll-*a* concentration at depth. Secondly, each point of the fluorescence profile is then multiplied by a correction coefficient which forces the Chlorophyll-*a* integrated content measured on the fluorescence profile to be consistent with the concomitant ocean color observation. The method is close to the approach proposed by Boss et al. (2008) to calibrate fluorescence data of a profiling float, although important differences do exist. To develop and test our approach, in situ data from three open ocean stations (BATS, HOT and DYFAMED) were used. Comparison of the so-called "satellite-corrected" fluorescence profiles with concomitant bottle derived estimations of Chlorophyll-*a* concentration was performed to evaluate the final error, which resulted to be of about 31 %. Comparison with the Boss et al. (2008) method, carried out on a subset of the DYFAMED data set simulating a profiling float time series, demonstrated that the methods have similar accuracy. Applications of the method were then explored on two different data sets. Using fluorescence profiles at BATS, we show that the integration of "satellite-corrected" fluorescence profiles in Chlorophyll-*a* climatologies could improve both the statistical relevance of Chlorophyll-*a*

BGD

8, 11899–11939, 2011

averages and the vertical structure of the Chlorophyll-*a* field. We also show that our method could be efficiently used to process, within near-real time, profiles obtained by a fluorometer deployed on autonomous platforms, in our case a bio-optical profiling float. The wide application of the proposed method should provide a first step toward the generation of a merged satellite/fluorescence Chlorophyll-*a* product, as the "satellite-corrected" profiles should then be consistent with satellite observations. Improved climatologies and more consistent satellite and in situ data (comprising those from autonomous platforms) should strongly enhance the performance of present biogeochemical models.

1 Introduction

The Total Chlorophyll-*a* (called "Chl-*a*" here, the sum of chlorophyll-*a*, divinyl chlorophyll-*a* and chlorophyllide-*a*) is the dominant photosynthetic pigment present in all autotrophic marine organisms. In the ocean, its concentration is considered a good, although not optimal, proxy for phytoplankton biomass (i.e. Cullen, 1982; Strickland, 1965). Considering the key role of phytoplankton in the global carbon cycle, understanding the Total Chl-*a* concentration ("[Chl-*a*]") spatio-temporal distribution and variability is on primary importance for modern oceanography (Claustre et al., 2010). However, as with several other biological parameters, observations of [Chl-*a*] are scarce, particularly in comparison with the number of physical observations available (i.e. temperature and salinity). Amongst the three main approaches that exists for measuring [Chl-*a*] (i.e. water sampling, ocean color and induced fluorescence, see later), fluorescence is undoubtedly the one which has been the least scientifically exploited. However, it represents the most important source of in situ data, in terms of numbers of observations (i.e. 36 707 profiles in the World Ocean Database 2009; Boyer et al., 2009), and this trend is likely to increase in the near future given the recent development of autonomous platforms equipped with fluorometers. Combining fluorescence profiles with other data (i.e. ocean color and sampling bottles) should strongly enhance

BGD
8, 11899–11939, 2011

our knowledge of the [Chl-*a*] spatio-temporal variability, and consequently, improve our comprehension of the phytoplankton dynamics.

The conventional and historical approach to measure [Chl-*a*] in the ocean is to filter water samples collected at different depths. These filters can then be analysed by a number of techniques, such as fluorometry, spectroscopy or chromatography, which have different degrees of accuracy and precision. The most accurate is definitively the High Performance Liquid Chromatography (HPLC; Gieskes and Kraay, 1983), which additionally provides the concentrations of a large spectrum of phytoplankton accessory pigments in addition to Chl-*a*.

There are also bio-optical techniques that offer alternative methods to obtain [Chl-*a*] in the ocean. Empirical relationships, relating the gradients in light field to in-water compounds, were developed to estimate [Chl-*a*] from radiometers that measure light intensity in the visible spectrum (Morel, 1988). Similarly, bio-optical relationships were successfully developed to obtain [Chl-*a*] from satellite-mounted radiometers. The satellite-derived maps provide a unique temporal and spatial picture of the [Chl-*a*] at global scale (Feldman et al., 1989; McClain et al., 1998). However, satellite observations are limited to the ocean surface and their error on [Chl-*a*], calculated by match-up analysis of concurrent satellite and HPLC measurements, was evaluated to vary around ± 35 % in the open ocean (Bailey and Werdell, 2006; Moore et al., 2009).

Bio-optical approaches based on fluorescence techniques (Lorenzen, 1966) provide another method to evaluate [Chl-*a*]. Irradiated by blue light, Chl-*a* re-emits, in the red part of the spectrum, a quantity of light, which is proportional to [Chl-*a*]. Based on this concept, instruments inducing and measuring fluorescence (i.e. fluorometers) provide a robust method to estimate in situ [Chl-*a*] with a non-invasive technique. Additionally, the acquisition frequency of fluorometers (up to 8 Hz) and their possible connection with a CTD probe, allows for winch-based deployment and the collection of vertically continuous profiles of fluorescence. Although calibration issues still prevent a wide scientific exploitation of fluorescence profiles (see later), during the last 30 years they have been extensively collected, becoming a standard measurement in oceanography.

BGD
8, 11899–11939, 2011

The calibration of fluorometers is a complex process. Manufacturer calibration is often too simplistic to meet scientific requirements, and calibration needs to be regularly verified, due to lamp and sensor performance degradation with time. However, the most problematic issues are the high variability and non-linearity of the fluorescence/Chl-*a* relationship (Falkowski and Kiefer, 1985; Kiefer, 1973). Changes in environmental conditions (i.e. light intensity, nutrient availability) can induce modifications in taxonomic assemblages or in physiological states of phytoplankton, with an impact on the fluorescence to Chl-*a* ratio (Cullen, 1982; Althuis et al., 1994; Claustre et al., 1999; Cleveland and Perry, 1987; Loftus and Seliger, 1975). An in situ calibration of the fluorometers is generally carried out at the time of deployment, using [Chl-*a*] obtained from water samples collected during the fluorescence profiles acquisition and further analyzed with HPLC or spectrofluorometer (Cetinic et al., 2009; Sharples et al., 2001; Strass, 1990). This operation, however, is not systematically carried out. Moreover, even when bottle data are available, they are often recorded in a different database to the fluorescence profiles. Consequently, in situ fluorescence profiles are only used to indicate a "generalized" biomass index (Strickland, 1968), interpreted to decide the depths for bottle sampling during a cruise. Occasionally, they are used to improve the interpolation of discrete [Chl-*a*] estimations from bottle sampling (Morel and Maritorena, 2001).

The main consequence of this situation is that fluorescence data are underused. The constraints of calibration hinder any combination of the different fluorescence data sets, but also prevents their merging with other data sources. No fluorescence profile has been integrated, for example, in existing [Chl-*a*] climatologies (Conkright et al., 2002), which are exclusively based on [Chl-*a*] estimations obtained from water sample data (HPLC or spectrofluorometer measurements). Consequently, climatologies are strongly interpolated, as the initial data density is generally low (Conkright et al., 2002). Furthermore, existing methods to generate blended [Chl-*a*] products combining data derived from different methods generally exclude fluorescence data. They have been limited to the merging of ocean color satellite observations with water sample-derived

BGD
8, 11899–11939, 2011

estimations. A pure blending method (Gregg and Conkright, 2001) was developed to directly merge satellite and in situ data. A more indirect approach used satellite and in situ data to establish empirical relationships between the surface [Chl-*a*] and its vertical signature (Morel and Berthon, 1989; Uitz et al., 2006), in order to reconstruct a vertical profile to each available satellite pixel. Surprisingly, no attempt yet exists to merge fluorescence profiles with alternative [Chl-*a*] measurement approaches.

In summary, the lack of homogenisation of the fluorescence calibration methods prevents the development of a merged procedure that makes use of a number of different fluorescence data sets and of their combination with other data sources.

To solve this issue, any utilisation of bottle derived [Chl-*a*] data, should be avoided. Along this line, recent approaches were presented, based on ancillary data (i.e. simultaneous irradiance profiles, Xing et al., 2011a), on the shape of fluorescence profile (Mignot et al., 2011) or on satellite ocean color [Chl-*a*] observations (Boss et al., 2008). The last method (Boss et al., 2008), although developed to calibrate a profiling float fluorometer, also points to a reliable way to merge fluorescence profiles and satellite observations. However, the Boss et al. (2008) approach, in its present form was developed to be applied to a time series of profiles performed by a single fluorometer deployed on a profiling float and is likely not suitable for other data sets. Indeed, a unique set of calibration factors was calculated for the whole life-time of the profiling float. Consequently, although the calibrated data are generally consistent with the satellite, the computation of a unique set of calibration factors implies that some profiles could be erroneously calibrated. In the framework of a combined satellite-fluorescence profile product, the present form of the Boss et al. (2008) method could then be modified in order to be applied on a single profile basis.

Here, we propose a method to merge fluorescence profiles and satellite ocean color observations, which is conceptually close to the Boss et al. (2008) procedure. The main difference is that it is applicable on a single profile basis. Consequently, each profile will be characterized by a specific set of calibration factors and the obtained [Chl-*a*] profiles would be strictly consistent with the satellite estimation measured in the

BGD
8, 11899–11939, 2011

same place and at the same time.

We developed and tested the merging method on three long term time-series of simultaneous observations of fluorescence profiles and [Chl-*a*] obtained from HPLC analysis. Fluorescence profiles and satellite data were matched and combined to generate [Chl-*a*] profiles. Finally, the obtained profiles were compared with concomitant HPLC [Chl-*a*], to test the method performances. Additionally, performance indexes of the present merging method were compared to the Boss et al. (2008) method performances on a subset of DYFAMED data. The different sources of error influencing the accuracy of the merged profiles were then discussed. Finally, two examples of application were presented: the production of a monthly [Chl-*a*] climatology using fluorescence profiles and the treatment of a time-series of fluorescence profiles recorded by a fluorometer deployed on a profiling float. The two applications demonstrate the capacity of the method to enhance the consistency of the fluorescence data set with other [Chl-*a*] data sources available. Consequently, they represent a first step towards a blending method of the [Chl-*a*] data estimations.

2 Data

In situ data from the long-term time-series data sets of stations BATS (Michaels and Knap, 1996, in the Sargasso Sea), DYFAMED (Marty et al., 2002, in the North Western Mediterranean Sea) and HOT (Karl and Lukas, 1996, in the North Pacific) were used. For each station, fluorescence, temperature and salinity profiles were extracted, as well as HPLC [Chl-*a*] derived from discrete samples, where available.

Surface [Chl-*a*] over the three sites were derived from the 8-day images at 9 km spatial resolution from the SeaWiFS satellite ocean color sensor, which constitutes the longest temporal series of ocean color observations (McClain, 2009). For each available fluorescence profile, the satellite image that matched the date of the profile was selected, and a [Chl-*a*] average was calculated in a $\pm 0.25^{\circ}$ by $\pm 0.25^{\circ}$ sized box centred on the profile geographical position (i.e. "fluo" match-up). A "fluo" match-up was retained, if more than 30 % of pixels were available in the box.

BGD
8, 11899–11939, 2011

For each station, an additional satellite match-up analysis was performed by extracting ocean color data when HPLC observations were available ("HPLC" match-up). To verify the sensitivity of the match-up analysis to the size of the temporal and spatial windows, near surface [Chl-*a*] from HPLC profiles (computed as described in Morel and Berthon, 1989) were compared to satellite observations extracted from SeaWiFS images at both 8-day and 1-day temporal resolution and on spatial boxes of $\pm 0.25^{\circ}$ and $\pm 0.1^{\circ}$ dimensions (Table 1). Increasing temporal and spatial resolutions does not significantly modify the similarity between the HPLC and satellite estimations. However, the number of match-ups strongly decreased. Based on these tests, carried out on the "HPLC" match-ups, the "fluo" match-up procedure was then performed using the 8-day resolution products and the $\pm 0.25^{\circ}$-square boxes.

For the three stations, only the HPLC and fluorescence data available for the 1998–2007 period were retained (i.e. the period of activity of the SeaWiFS ocean color sensor). In the BATS and DYFAMED HPLC data sets, the lowest [Chl-*a*] were around $0.001\,\mathrm{mg\,m^{-3}}$ whereas at the HOT station lowest concentrations were about $0.01\,\mathrm{mg\,m^{-3}}$. As observations showed that in the most oligotrophic regions of the global ocean, [Chl-*a*] at the surface is about $0.02\,\mathrm{mg\,m^{-3}}$ (Ras et al., 2008), very low [Chl-*a*] ($< 0.01\,\mathrm{mg\,m^{-3}}$) should correspond to deep measurements that are not relevant to this present study. Consequently, to homogenise the data sets, we eliminated all the HPLC measurements $< 0.01\,\mathrm{mg\,m^{-3}}$.

On the HPLC profiles, negative spikes (2 % of total HPLC data points) and incomplete profiles (i.e. less than 5 points, 2.2 % of available profiles) were also removed. An additional quality control procedure (D'Ortenzio et al., 2010) was applied to the fluorescence profiles, which checked for outliers, spikes and unexpected gradients. Finally, an additional visual control allowed for the identification of altered profiles which were removed.

After this processing, the fluorescence database was composed of 3804 profiles, all with an associated satellite ocean color [Chl-*a*] estimation: 93 at DYFAMED, 1662 at HOT, 2049 at BATS (see Table 2 to a summary of the available data).

BGD
8, 11899–11939, 2011

3 Method

3.1 Overview

The common procedure to convert a fluorescence profile (FLUO) into [Chl-*a*] (Boss et al., 2008; Cetinic et al., 2009; Xing et al., 2011a) can be formalised by:

$$[\text{Chl}-a] = \alpha(\text{FLUO}-\beta) \quad (1)$$

The β parameter indicates the response of the instrument in the absence of signal and it is commonly computed by blocking the sensor window. The α coefficient is initially provided by the manufacturer and it is calculated by linear regression with samples at fixed and known [Chl-*a*]. Post-processing evaluation of the α parameter can be carried out by regressing fluorescence profiles with in situ [Chl-*a*] obtained by HPLC or spectrofluorometer water sample analyses. The post-processing calibration is generally more accurate than the manufacturer calibration, as it is often carried out in natural conditions and on a greater number of data points. However, it requires the analysis of water samples, which are not always available.

Here, we evaluated the β parameter by considering fluorescence measurements at depth, where [Chl-*a*] is supposed to be zero, whereas the α parameter was estimated for each fluorescence profile from a simultaneous ocean color observation.

The evaluation of the α parameter was based on the relationship between the near-surface [Chl-*a*], $[\text{chl}]_{\text{surf}}$, and the integrated Chl-*a* biomass across k times the euphotic layer, $\langle\text{chl}\rangle_{k.Z_e}$, ($k = 1$ or $k = 1.5$; Morel and Berthon, 1989; Uitz et al., 2006):

$$\langle\text{chl}\rangle_{k.Z_e} = A[\text{chl}]^B_{\text{surf}} \quad (2)$$

where, A and B are coefficients which were determined by regressions carried out on in situ data (Table 3; Uitz et al., 2006). A and B have different values depending whether the water column is stratified or not.

BGD
8, 11899–11939, 2011

3.2 Parameters computation

Following Morel and Berthon (1989) and Uitz et al. (2006), the discrimination between a stratified or mixed water column was determined according to the ratio between the depth of the euphotic layer (Z_e) and the depth of the mixed layer (Z_m). The water column was assumed to be mixed when $Z_e/Z_m < 1$ and stratified when $Z_e/Z_m > 1$. Z_m was evaluated from potential density profiles using a density criterion of 0.03 kg m^{-3} (de Boyer Montegut et al., 2004; D'Ortenzio et al., 2005). Z_e was determined with the following procedure: (1) the attenuation coefficient at 490 nm, K_{d490}, from the satellite derived [Chl-*a*] (Morel and Maritorena, 2001); (2) the total attenuation coefficient, K_d, from K_{d490} (Rochford et al., 2001); (3) finally, Z_e was retrieved from K_d, using the equations of exponential decrease of light over depth.

Before computing the α and β parameters, fluorescence profiles were corrected for non photochemical quenching (NPQ). NPQ generally occurs in the surface layer, where, in response to supra-optimal light irradiation, phytoplankton triggers photo-protection mechanisms, inducing a drastic decrease of the fluorescence to [Chl-*a*] ratio (Kolber and Falkowski, 1993; Müller et al., 2001). NPQ represents a serious issue for the fluorescence calibration (Cullen and Lewis, 1995; Xing et al., 2011a) but correction methods exist. Here, we used the method proposed by Xing et al. (2011b), which consists in extrapolating up to the surface, the highest fluorescence value encountered within the mixed layer.

The coefficient β was evaluated under the hypothesis that [Chl-*a*] was equal to zero in deep waters:

$$\beta = \text{average}(\text{FLUO}(z)), \text{ for } z > Z_{\text{threshold}} \quad (3)$$

where z is the depth in meters and $Z_{\text{threshold}}$ is a depth below which the [Chl-*a*] was considered null. Here, we assumed that $Z_{\text{threshold}} = 300$ m, for stratified water columns, and $Z_{\text{threshold}} = Z_m + 100$ m, for mixed water columns.

The α parameter for each fluorescence profile was, subsequently, determined thanks to ocean color satellite measurements. First, using Eq. (2) and Table 3, the

BGD
8, 11899–11939, 2011

near-surface [Chl-*a*], measured by satellite sensor, was related to the integrated Chl-*a* content over $1.5Z_e$, $\langle chl \rangle_{1.5Z_e}$ (Morel and Berthon, 1989; Uitz et al., 2006). Then, the fluorescence profile, corrected for NPQ effect, was adjusted so that $\langle chl \rangle_{1.5Z_e}$ and the integrated Chl-*a* measured by fluorescence coincide. α was accordingly computed as followed:

$$\alpha = \frac{\langle chl \rangle_{1.5Z_e}}{\int_0^{1.5Z_e} (FLUO(z) - \beta) dz} \quad (4)$$

Note that we used integrated content over $1.5Z_e$ because it is recognized that an important phytoplankton biomass is often present below the euphotic layer (Uitz et al., 2006).

The estimation of the parameters α and β was carried out for each available fluorescence profile of the three stations, and, using Eq. (1), ocean color/fluorescence merged profiles were finally obtained (thereafter "satellite-corrected" profiles).

3.3 Statistics used to asses method performances

To evaluate the method various statistics were computed on couples of concomitant [Chl-*a*] derived from both "satellite-corrected" profiles and HPLC estimations, the last being considered as the "true" value. The two series of [Chl-*a*] estimations (i.e. "satellite-corrected" and HPLC) were matched according to the station, the sampling day and the depth.

The median value of ratio "satellite-corrected" to HPLC [Chl-*a*] estimations points to the overall bias. The semi interquartile range (SIQR) provides insight on the spreading of data and it is defined as:

$$SIQR = \frac{Q_3 - Q_1}{2} \quad (5)$$

where Q_1 is the 25th percentile and Q_3 is the 75th percentile of each series of "satellite-corrected" to HPLC ratio.

BGD
8, 11899–11939, 2011

The median percent difference (MPD) was calculated to measure how accurately the [Chl-*a*] values of the "satellite-corrected" profiles agree with HPLC measurements. It is defined as the median of the individual absolute percent differences (PD), computed as:

$$\mathrm{PD}_i = 100\frac{|X_i - Y_i|}{Y_i} \quad (6)$$

where Y_i is the [Chl-*a*] measured with HPLC of the ith validation point and X_i is the corresponding "satellite-corrected" value. The determination coefficients (r^2) of linear regression between "satellite-corrected" and HPLC estimations were also evaluated.

4 Results

4.1 Method performances

The four terms (i.e. median "satellite-corrected" to HPLC ratio, SIQR, MPD and r^2) described in the Sect. 3.3 were calculated for complete data sets of 2667 pairings of concurrent "satellite-corrected" with HPLC [Chl-*a*] (500 for DYFAMED, 1030 for BATS and 1137 for HOT). Because of the log-normal distribution of [Chl-*a*], values were log-transformed (Campbell, 1995) prior to statistical analysis, except for the PD calculation.

Statistics and scatter plots are shown in Table 4 and Fig. 1, for each station. Figure 2 shows some examples of the initial fluorescence profiles, with their corresponding "satellite-corrected" and HPLC profiles. In Fig. 2, the satellite surface [Chl-*a*] used for merging is also depicted, as well as the "HPLC-calibrated" profiles, computed by adapting the initial fluorescence profiles to the simultaneously available discrete HPLC observations (following the method of Morel and Maritorena, 2001).

The scattering of data for the three stations is relatively homogenous around the 1 : 1 line for each station (Fig. 1, panels a to c) but also for surface data (< 20 m, Fig. 1, panel d) suggesting that the NPQ-correction applied here was globally efficient. The present

BGD
8, 11899–11939, 2011

merging method does not appear biased, as median values of the "satellite-corrected" to HPLC ratio are within 5 % of a unit (Table 4). A significant scatter, especially at the DYFAMED station, is, however, observed with SIQR, ranging from 0.15 to 0.29. The MPD ranges from 28 % for station HOT to 41 % for DYFAMED, with an overall median value of 31 %. Determination coefficients range from 0.62 for BATS to 0.70 for DYFAMED station. Not surprisingly, r^2 is higher in stations where large ranges of [Chl-*a*] are observed (i.e. DYFAMED).

The precision of the satellite observation used to calculate the α parameter impacts on the accuracy of the "satellite-corrected" profiles at stations DYFAMED and BATS (Table 5). Indeed, the performance of the method increases, when the satellite observations are accurate (i.e. difference between satellite and HPLC surface values less than ± 30 %, Table 5 and examples on Fig. 2, panels a and b). Otherwise, the performance of the method is quite poor (examples on Fig. 2, panels c and f). However, the impact of satellite error on the final "satellite-corrected" [Chl-*a*] estimations is minimised. This effect is particularly evident at station HOT where the final error is set around 28 %, regardless of the initial satellite error. Standardisation of error could be ascribed to the smoothing effect relative to the utilization of integrated Chl-*a* contents instead of surface values in the determination of the α parameter.

A comparison of the vertically integrated [Chl-*a*] was also performed (Fig. 3). [Chl-*a*] of both "satellite-corrected" and "HPLC-calibrated" profiles were integrated over 200 m depth, which generally corresponds to the deepest HPLC observation. Moreover, at 200 m depth, [Chl-*a*] is in most cases considered to be close to zero. For the integrated [Chl-*a*], the median of "satellite-corrected" to "HPLC-calibrated" ratio is 1.06, SIQR is 0.22 and median error is 20.0 %. Determination coefficient in the regression model only reaches 53 %, indicating a relatively weak coherence between the data sets, which is particularly evident for low values. Again, satellite accuracy impacts on the final result. Underestimation (overestimation) of the satellite surface [Chl-*a*] directly results in an underestimation (overestimation) of the integrated content of the "satellite-corrected" profiles. Nevertheless, the impact is less significant than expected: of the 144 profiles

BGD
8, 11899–11939, 2011

with an error on satellite [Chl-*a*] higher than 30 %, about half (82 profiles) showed integrated chlorophyll contents close to their corresponding HPLC calibrated profiles (error less than 30 %).

Finally, we compared the euphotic depths calculated from the "satellite-corrected" and from the "HPLC-calibrated" profiles, following the method of Morel and Berthon (1989) but with the parameterisation of Morel and Maritorena (2001, Fig. 4). Note that the euphotic depth is an important parameter of our approach since it was used to evaluate the layer of integration in Eq. (4) and to establish whether the water column is stratified or mixed. The points are uniformly scattered around the 1:1 line. Similarly to the analysis of integrated [Chl-*a*], it appears that the satellite error tends to affect the estimation of Z_e in "satellite-corrected" profiles. However, the correlation between "satellite-corrected" and "HPLC-calibrated" Z_e is satisfying (median ratio of "satellite-corrected" to "HPLC-calibrated" = 0.97, SIQR = 0.09, MPD = 9.5 %, $r^2 = 0.64$).

4.2 Comparison with the method proposed by Boss et al. (2008)

Even though differences exist, our approach is close to the Boss et al. (2008) fluorescence correction method. Both methods use a satellite reference, except that the Boss et al. (2008) approach was developed to be applied to a set of fluorescence profiles measured by a unique instrument (i.e. profiling float), free of instrumental drift. To verify the performances of both approaches, we selected a subset of data from the DYFAMED data set, in order to be as close as possible to the terms of applicability of the Boss et al. (2008) method (i.e. data obtained by a unique instrument). The DYFAMED subset of profiles was obtained by a single fluorometer from 2000 to 2002. To verify that there was no instrumental drift during this period, the deep fluorescence values have been checked (i.e. deep values between a standard deviation from the long term mean). The resulting subset of DYFAMED data comprises 47 fluorescence profiles, 24 of whom were associated to a concomitant HPLC profile.

By definition, the coefficients α and β in the Boss et al. (2008) approach (called α_B and β_B hereafter) were considered constant. Using the 47 profiles available, β_B was

BGD
8, 11899–11939, 2011

computed using the median value of the β coefficients computed with our method. The α_B coefficient was calculated as the type II regression slope of a regression analysis performed between surface satellite [Chl-*a*] and the corresponding surface values of fluorescence profiles. Note, however, that the satellite [Chl-*a*] product that we used has different spatial (9 km instead of 1 km in Boss et al., 2008) and temporal (8-day instead of 1-day) resolutions.

The comparison of "satellite-corrected" and "Boss-calibrated" profiles (i.e. fluorescence profiles calibrated with the Boss et al., 2008, method) with concomitant HPLC [Chl-*a*] estimations (Table 6, 224 validation points) indicates that the performance indexes of both methods are equivalent (MPD = 43.5 % with the present method and 42.7 % with the Boss et al., 2008, method). Dispersion is slightly reduced with the Boss et al. (2008) method compared with the present merging method (SIQR = 0.24 against 0.27 with our method and $r^2 = 0.87$ against 0.77). Also, our merging method seems more sensitive to the accuracy of satellite data (see example on Fig. 2, panels c and d).

4.3 Examples of application

4.3.1 Chlorophyll-*a* climatology

The utilisation of the large data set of fluorescence profiles, once properly calibrated, should strongly improve the existing climatologies, for two specific aspects in particular:

1. The increased number of values for each grid box could improve the statistical relevance and the accuracy of the averaged [Chl-*a*] at a given depth. To verify this point, we linearly interpolated the HPLC discrete profiles on the vertical scale to generate continuous profiles at 1 m resolution. Twelve monthly HPLC average values were then calculated over standard depths, defined for each station by considering the most recurrently sampled depths. At each standard depth, monthly climatological means were also computed by averaging, for a given month, the [Chl-*a*] extracted from the "satellite-corrected" profiles. The resulting mean values

BGD
8, 11899–11939, 2011

were finally compared with the HPLC derived estimations (Fig. 5 and Table 7). Resulting statistics are generally improved (see Table 7): SIQR is 0.11 (instead of 0.16 for the single profile application), MPD is 21 % (instead of 31 %) and r^2 is 0.82 (instead of 0.67). HPLC to "satellite-corrected" data spreading is also reduced and points are aligned over the first bisector. However, as also observed for the single profile comparison, dispersion increases for concentrations lower than 0.05 mg m^{-3}.

2. The utilisation of "satellite-corrected" profiles led us to envisage new types of climatologies which could better reproduce the vertical distribution of [Chl-*a*]. A new procedure is proposed here, (see Appendix A for computation details). Briefly, the procedure tends to identify, in all available [Chl-*a*] profiles, relevant features of the profile, such as the DCM depth, and averages them to reconstruct a climatological profile which depicts the main characteristics of typical [Chl-*a*] profiles. Such a procedure is, consequently, based on the a-priori knowledge of the typical shapes of [Chl-*a*] profiles and does not allow the merging of two [Chl-*a*] profiles which have different shapes. Here, we distinguished [Chl-*a*] profiles marked by a DCM and attributed to stratified water columns to homogeneous profiles characterising the mixed water columns (Mignot et al., 2011). As an example, this procedure was applied to the BATS "satellite-corrected" profiles (Fig. 6). Comparing the new climatology with a climatology based on HPLC discrete samples (Fig. 6), we observed that the marked seasonality of the [Chl-*a*] field, characteristic of the region (Steinberg et al., 2001), is well reproduced in both climatologies. When most of [Chl-*a*] profiles have a stratified shape (i.e. April to December), the two climatologies agree at surface and below the DCM. However, the HPLC-based climatology shows shallower and weaker DCMs than those observed in the so called fluorescence-based climatology, particularly in spring. When the mixed situation dominates (i.e. January to March), the fluorescence-based climatological profiles are constant in surface layers (0–100 m), whereas HPLC-based climatological profiles display a sub-surface maximum.

BGD
8, 11899–11939, 2011

4.3.2 Autonomous platforms

The merging method was then applied to calibrate NPQ corrected fluorescence data obtained from a PROVBIO, an Argo-like profiling float equipped with a fluorometer (Xing et al., 2011a). The float was deployed in the Eastern Mediterranean Sea, collecting 90 profiles between the 27 June 2008 and the 8 November 2009. As the SeaWiFS sensor was sometimes deficient during the 2008/2009 period, satellite data extraction was achieved using MODIS 8-day data. The time-series of "satellite-corrected" profiles is presented in Fig. 7, panel a. A well marked seasonal cycle, consistent with previous observations of Krom et al. (1992) is observed. This cycle presents a strong stratification of the water column in summer, characterized by a DCM between 100 and 125 m depth. During winter, [Chl-*a*] is quite constant throughout the mixed layer, which deepens to more than 250 m in February/March 2009. [Chl-*a*] values never exceed 0.68 mg m^{-3}. The maxima are observed at the DCM (summer 2008, spring 2009), in agreement with the well known characteristics of the Mediterranean oligotrophic areas (Moutin and Raimbault, 2002).

For the sake of comparison, the modified Boss et al. (2008) method (see Sect. 4.2) was also applied (Fig. 7, panel b). The two series of profiles are consistent from July to September 2008, with [Chl-*a*] ranges between 0 and 0.65 mg m^{-3}. Significant differences are however observed for the rest of the period (from October 2008 to October 2009), when the "Boss-calibrated" [Chl-*a*] is significantly lower (on average 0.15 mg m^{-3} difference at DCM).

5 Discussion

Compared with HPLC references, "satellite-corrected" fluorescence profiles are globally unbiased, although presenting a significant scatter ($r^2 \sim 67\,\%$) and an important median error ($\sim 31\,\%$). These errors (Figs. 1, 3 and 4, Table 5) are certainly affected by the uncertainty of satellite [Chl-*a*] measurements, estimated less than 35 %

BGD
8, 11899–11939, 2011

in oligotrophic ocean gyres (Moore et al., 2009). Nevertheless, it is even more relevant within certain localised areas (i.e. the Mediterranean Sea, D'Ortenzio et al. 2002; the Antarctic or the Equatorial Atlantic, Gregg and Casey, 2004). The matchup procedure used to associate a satellite observation to a fluorescence profile could also impact on the final [Chl-*a*] profile. However, a narrower matchup protocol (i.e. 1-day and/or $0.1^{\circ} \times 0.1^{\circ}$ box) does not significantly enhance the performance (Table 1), although, conversely, it does decrease the number of available satellite observations, (cloud cover limits the satellite coverage in the match up box) and, therefore, their statistical relevance.

Another potential source of error derives from the conversion of surface [Chl-*a*] into integrated Chl-*a* content over the water column, (Eq. 2 as obtained by regression analyses performed by Uitz et al., 2006). However, the use of vertically integrated contents to calculate the calibration coefficients, i.e. Eq. (4), does not change the method performance, when compared with HPLC estimations (Table 6). We suppose that integrating over the $1.5Z_e$ decreases the impact of the vertical variability of the Chl-*a*/fluorescence ratio on the final calculation of α. Additionally, using integrated contents, the α calculation is less affected by the method of NPQ correction.

A possible alternative to Eq. (2) is the use of surface measurements, as proposed by Boss et al. (2008). In this case, however, the variability of the Chl-*a*/fluorescence relationship could have a larger impact on the final profile, as a possible error in the surface data should propagate all along the water column. Moreover, for surface observations, the accuracy of the NPQ correction (i.e. surface measurements are more affected by NPQ than deep values) and of the satellite estimations is likely crucial. On our data sets test, however, these effects seem minimized (Table 6) and we suppose that this is mainly due to the statistical significance of the regression used to calculate α_B ($p_{\text{value}} = 2.10^{-7}$ for the DYFAMED subset). If the statistical relevance of the regression to calculate α_B had been low (i.e. few match-ups, important satellite errors, regional biases), even profiles having a good satellite match-up would have been erroneously calibrated.

BGD
8, 11899–11939, 2011

The Boss et al. (2008) method therefore represents a powerful tool, and a valid alternative, to calibrate fluorescence profiles and to produce vertical estimations of [Chl-*a*] consistent with satellite data. Our method is merely an improvement of the Boss et al. (2008) method. The main methodological differences between the two approaches seem to have a very weak impact on the final errors (Table 6) and the two methods appear equivalent from the point of view of the error analysis. However, the Boss et al. (2008) method was specifically developed to derive an accurate estimation of [Chl-*a*] from fluorescence measurements performed by a profiling float, which was (1) equipped with a unique fluorometer, (2) spanning on a three-year period only, (3) floating in a limited, although vast, ocean region (i.e. Western North Atlantic). For this reason, their method was based on a unique calibration factor for all the series of profiles and, to match satellite observations, they used only surface data.

Our objective has been to enhance the Boss et al. (2008) method so as to be able to process any fluorescence profile having a concurrent satellite observation (i.e. after 1997). Consequently, we decided to (1) generate a calibration factor for each profile (2) enlarge the temporal and spatial window of the satellite observations, to ensure a match-up, even in regions with low satellite coverage and (3) use $1.5Z_e$ integration depth instead of surface points only, to minimize the effect of the error propagation along the vertical scale in case of high vertical variability of the Chl-*a*/fluorescence ratio. We are confident that, with these characteristics, our method could be widely applied (i.e. to all fluorescence profiles in the NODC data base collected after 1997). Furthermore, the calibrated data set of fluorescence profiles could be used to generate a satellite/fluorescence blended product of the [Chl-*a*].

The potential of this blended product are evident for the generation of a new type of climatology of [Chl-*a*]. Compared with a climatology generated with only discrete samples (i.e. HPLC), the new fluorescence-based climatology exhibits some differences, mainly in the mixed layer and at the DCM (Fig. 6). The causes of these discrepancies must be ascribed to methodological issues. In particular, climatologies based on HPLC discrete points generally require interpolations on the vertical scale, which could

BGD
8, 11899–11939, 2011

smooth the final mean profile (see for example Fig. 6). Additionally, averaging mixed and stratified profiles generates atypical shapes (see winter months of the HPLC-based climatology at BATS, Fig. 6), which have no correspondence with the initial data set, but are pure artefacts of the mean procedure. In the new fluorescence-based climatology (Fig. 6), the dominant shape (i.e. stratified or mixed) appears more clearly and the proposed method to calculate the climatological profile results in marked DCM peaks, as generally expected.

The merging method proposed here has also been applied to a profiling float fluorometer and the obtained results were compared with those derived from the method of Boss et al. (2008), which was specifically developed for profiling float data. The application of the two procedures on a single set of fluorescence profiles leads to significantly different results (Fig. 7). At the present stage, it is impossible to definitely assess which method is closest to the truth. However, both the methods are consistent, by definition, with the concurrent satellite estimations. In other words, the profiling float observations could be easily merged with satellite ocean colour maps, to finally generate a unique 3-D picture of the [Chl-*a*] field. The use of this 3-D picture of [Chl-*a*] could significantly improve the operational simulations of oceanic ecosystems, in particular in an assimilation scheme (Brasseur et al., 2009). In this context, our method appears more promising than the Boss et al. (2008) procedure, which rather requires the utilisation of all the fluorescence profiles achieved during the whole life-time of the float to determine calibration coefficients, and thus which cannot be applied in a real-time.

6 Conclusions

We have presented a method to merge fluorescence profiles and satellite ocean color observations, which allows for a homogenisation of the existing [Chl-*a*] estimations derived from fluorescence observations. Fluorescence profiles, obtained from a range of fluorometers and factory calibrations and under various trophic and environmental conditions, were calibrated on a unique and stable reference provided by ocean color

BGD
8, 11899–11939, 2011

satellites. Consequently, for the first time, the huge data set of fluorescence profiles collected during the last 15 years could be inter-compared. Moreover, the calibrated fluorescence profiles being consistent with satellite observations, their integration and merging with other data sources should be strongly facilitated.

The limits of the present method are essentially determined by the limits of the data sets used (i.e. fluorescence and satellite observations). If no satellite match-ups are available, a merging procedure cannot be performed. Consequently, all fluorescence profiles performed before 1997 (date of launching of the SeaWiFS sensor), as well as profiles achieved in high latitudes, cannot be merged with satellite data. Biases are also induced by the error of satellite ocean color, which represents the first source of error of our method. However, the error estimated by comparing "satellite-corrected" fluorescence profiles with HPLC estimations, is only slightly higher than the error estimated for the ocean color satellite observations.

Although we accept that the merging method presented here cannot substitute, in terms of accuracy, the calibrations derived from laboratory analyses to determine [Chl-*a*], it does, nevertheless, present specific advantages, which could be particularly adapted for specific applications. We presented here two examples: the improvement of the [Chl-*a*] climatology and the treatment of fluorescence data measured by a profiling float. These two applications will probably converge in the future: at the present time, the only climatology available (Conkright et al., 2002) is based on discrete bottle data and suffers from (1) a critical lack of data and (2) a really poor vertical resolution. Integrating existing "satellite-corrected" fluorescence profiles in [Chl-*a*] climatologies should help in filling these gaps. Moreover, the high flux of fluorescence data provided by the increased number of profiling floats will definitively reinforce our capacity for describing, climatologically and in real time, the [Chl-*a*] field.

BGD
8, 11899–11939, 2011

Appendix A

Procedure to generate the new, fluorescence-based, [Chl-*a*] climatology

1. All the fluorescence profiles available for a given month were sorted into two categories: stratified and mixed with respect to the Z_m/Z_e ratio. If $Z_m/Z_e > 1$, the profile is associated to the mixed category, otherwise, it is associated to in the stratified category.

2. On one hand, the climatological profile representing the stratified category was computed as follows, (a) on each stratified profile, the DCM was identified as the absolute maximum on the vertical scale; (b) the profile depths were normalized by the depth of the DCM; (c) all the depth-normalized profiles were then averaged, for each unity of the dimensionless vertical scale; (d) the resulting mean profile was finally reconverted to a metric scale, using a multiplicative factor obtained by averaging the DCM depths of all the profiles. On the other hand, the climatogical profile corresponding to the mixed category was computed in a similar way as the climatological stratified profile except that the DCM depth used for normalization was replaced by the mixed layer depth.

3. Finally, only the climatological profile corresponding to the more frequent category (stratified or mixed) was retained to represent the monthly climatological [Chl-*a*] distribution.

Acknowledgements. The authors would like to thank all the staff of the DYFAMED observation service and of the BATS and HOT programs for the periodic measurements of oceanographic variables, and for the free distribution of data online. The US NASA space agency is thanked for the easy access to SeaWiFS and MODIS data. The authors are also grateful to Louis Prieur and Alexandre Mignot, for constructive comments and suggestions, to Joséphine Ras for reviewing the manuscript and to Emmanuel Boss (Univ. of Maine) who kindly provided details about his method. This paper is a contribution to the PABIM (Plateformes Autonomes Biogéochimiques: Instrumentation et Mesures) project funded by the Groupe Mission Mercator

BGD
8, 11899–11939, 2011

Coriolis (GMMC), to the PABO (Plateformes Autonomes and Biogéochimie Océanique) project funded by Agence Nationale de la Recherche (ANR) and to the remOcean (REMotely sensed biogeochemical cycles in the OCEAN) project, funded by the European Research Council (ERC).

The publication of this article is financed by CNRS-INSU.

References

Althuis, I. A., Gieskes, W. W. C., Villerius, L., and Colijn, F.: Interpretation of fluorometric chlorophyll registrations with Algal pigment analysis along a ferry transect in the Southern North Sea, Neth. J. Sea Res., 33(1), 37–46, 1994.

Bailey, S. and Werdell, P.: A multi-sensor approach for the on-orbit validation of ocean color satellite data products, Remote Sens. Environ., 102(1–2), 12–23, doi:10.1016/j.rse.2006.01.015, 2006.

Boss, E., Swift, D., Taylor, L., Brickley, P., Zaneveld, R., Riser, S., Perry, M., and Strutton, P.: Observations of pigment and particle distributions in the Western North Atlantic from an autonomous float and ocean color satellite, Limnol. Oceanogr., 53(5), 2112–2122, doi:10.4319/lo.2008.53.5_part_2.2112, 2008.

Boyer, T., Antonov, J., Baranova, O., Garcia, H., Johnson, D., Locarnini, R., Mishonov, A., O'Brien, T., Seidov, D., Smolyar, I., and Zweng, M.: World Ocean Database 2009, in: NOAA Atlas NESDIS 66, edited by: Levitus, S., US Gov. Printing Office, Washington, DC, 216 pp., DVDs, 2009.

de Boyer Montegut, C., Madec, G., Fischer, A., Lazar, A., and Iudicone, D.: Mixed layer depth

BGD
8, 11899–11939, 2011

over the global ocean: an examination of profile data and a profile-based climatology, J. Geophy. Res.-Oceans, 109(C12), C12003, doi:10.1029/2004JC002378, 2004.
Brasseur, P., Gruber, N., Barciela, R., Brander, K., Doron, M., El Moussaoui, A., Hobday, A., Huret, M., Kremeur, A., Lehodey, P., Matear, R., Moulin, C., Muturgudde, R., Senina, I., and Svendsen, E.: Integrating biogeochemistry and ecology into ocean data assimilation systems, Oceanography, 22(3), 206–215, 2009.
Campbell, J. W.: The lognormal distribution as a model for bio-optical variability in the sea, J. Geophys. Res., 100(C7), 13237–13254, doi:199510.1029/95JC00458, 1995.
Cetinic, I., Toro-Farmer, G., Ragan, M., Oberg, C., and Jones, B.: Calibration procedure for Slocum glider deployed optical instruments, Opt. Express, 17(18), 15420–15430, 2009.
Claustre, H., Morel, A., Babin, M., Cailliau, C., Marie, D., Marty, J.-C., Tailliez, D., and Vaulot, D.: Variability in particle attenuation and chlorophyll fluorescence in the Tropical Pacific: scales, patterns, and biogeochemical implications, J. Geophys. Res., 104(C2), 3401–3422, 1999.
Claustre, H., Antoine, D., Boehme, L., Boss, E., D'Ortenzio, F., Fanton D'Andon, O., Guinet, C., Gruber, N., Handegard, N. O., Hood, M., Johnson, K., Lampitt, R., LeTraon, P.-Y., Lequéré, C., Lewis, M., Perry, M.-J., Platt, T., Roemmich, D., Testor, P., Sathyendranath, S., Send, U., and Yoder, J.: Guidelines towards an integrated ocean observation system for ecosystems and biogeochemical cycles, in: Proceedings of OceanObs'09: Sustained Ocean Observations and Information for Society (Vol. 2), Venice, Italy, 21–25 September 2009, edited by: Hall, J., Harrison, D. E., and Stammer, D., ESA Publication WPP-306, doi:10.5270/OceanObs09.pp.14, 2010
Cleveland, J. S. and Perry, M. J.: Quantum yield, relative specific absorption and fluorescence in nitrogen-limited Chaetoceros gracilis, Mar. Biol., 94(4), 489–497, 1987.
Conkright, M., O'Brien, T., Stephens, K., Locarnini, R., Garcia, H., Boyer, T., and Antonov, J.: World Ocean Atlas 2001, Volume 6: Chlorophyll, edited by: Levitus, S., NOAA Atlas NESDIS 54, US Governement Printing Office, Washington, DC, 46 pp., 2002.
Cullen, J.: The deep chlorophyll maximum – comparing vertical profiles of chlorophyll-*a*, Can. J. Fish. Aquat. Sci., 39(5), 791–803, 1982.
Cullen, J. and Lewis, M.: Biological processes and optical measurements near the sea surface: some issues relevant to remote sensing, J. Geophy. Res.-Oceans, 100(C7), 13255–13266, 1995.
D'Ortenzio, F., Marullo, S., Ragni, M., Ribera d'Alcalà, M., and Santoleri, R.: Validation of empirical SeaWiFS algorithms for chlorophyll-*a* retrieval in the Mediterranean Sea: a case study

BGD
8, 11899–11939, 2011

for oligotrophic seas, Remote Sens. Environ., 82(1), 79–94, doi:16/S0034-4257(02)00026-3, 2002.
D'Ortenzio, F., Iudicone, D., Montegut, C., Testor, P., Antoine, D., Marullo, S., Santoleri, R., and Madec, G.: Seasonal variability of the mixed layer depth in the Mediterranean Sea as derived from in situ profiles, Geophys. Res. Lett., 32(12), L12605, doi:10.1029/2005GL022463, 2005.
D'Ortenzio, F., Thierry, V., Eldin, G., Claustre, H., Testor, P., Coatanoan, C., Tedetti, M., Guinet, C., Poteau, A., Prieur, L., Lefevre, D., Bourin, F., Carval, T., Goutx, M., Garçon, V., Thouron, D., Lacombe, M., Lherminier, P., Loisel, H., Mortier, L., and Antoine, D.: White Book on Oceanic Autonomous Platforms for Biogeochemical Studies: Instrumentation and Measure (PABIM) version 1.3, available at: http://www.obs-vlfr.fr/OAO/file/PABIM_white_book_version1.3.pdf, last access: 2011/12/06, 2010.
Falkowski, P. and Kiefer, D. A.: Chlorophyll-*a* fluorescence in phytoplankton: relationship to photosynthesis and biomass, J. Plankton Res., 7(5), 715–731, 1985.
Feldman, G., Kuring, N., Ng, C., Esaias, W., McClain, C., Elrod, J., Maynard, N., and Endres, D.: Ocean color: Availability of the global data set, Eos Trans. AGU, 70(23), 634, doi:10.1029/89EO00184, 1989.
Gieskes, W. W. and Kraay, G. W.: Unknown Chlorophyll-*a* derivatives in the North Sea and the Tropical Atlantic ocean revealed by HPLC analysis, Limnol. Oceanogr., 28(4), 757–766, 1983.
Gregg, W. W. and Casey, N. W.: Global and regional evaluation of the SeaWiFS chlorophyll data set, Remote Sens. Environ., 93(4), 463–479, doi:10.1016/j.rse.2003.12.012, 2004.
Gregg, W. W. and Conkright, M.: Global seasonal climatologies of ocean chlorophyll: blending in situ and satellite data for the coastal zone color scanner era, J. Geophy. Res.-Oceans, 106(C2), 2499–2515, 2001.
Karl, D. M. and Lukas, R.: The Hawaii Ocean Time-series (HOT) program: background, rationale and field implementation, Deep-Sea Res. Pt. II, 43(2–3), 129–156, doi:16/0967-0645(96)00005-7, 1996.
Kiefer, D. A.: Fluorescence properties of natural phytoplankton populations, Mar. Biol., 22(3), 263–269, 1973.
Kolber, Z. and Falkowski, P. G.: Use of active fluorescence to estimate phytoplankton photosynthesis in situ, Limnol. Oceanogr., 38(8), 1646–1665, 1993.
Krom, M., Brenner, S., Kress, N., Neori, A., and Gorgon, L.: Nutrient dynamics and new produc-

BGD
8, 11899–11939, 2011

tion in a warm-core eddy from the Eastern Mediterranean-sea, Deep-Sea Res., 39(3–4A), 467–480, 1992.
Loftus, M. and Seliger, H.: Some limitation of the in vivo fluorescence technique, Chesapeake Sci., 16(2), 79–92, 1975.
Lorenzen, C. J.: A method for the continuous measurement of in vivo chlorophyll concentration, Deep-Sea Res., 13, 223–227, 1966.
Marty, J.-C., Chiavérini, J., Pizay, M.-D., and Avril, B.: Seasonal and interannual dynamics of nutrients and phytoplankton pigments in the Western Mediterranean Sea at the DYFAMED time-series station (1991–1999), Deep-Sea Res. Pt. II, 49(11), 1965–1985, doi:16/S0967-0645(02)00022-X, 2002.
McClain, C. R.: A decade of satellite ocean color observations, Annu. Rev. Marine Sci., 1(1), 19–42, doi:10.1146/annurev.marine.010908.163650, 2009.
McClain, C., Cleave, M., Feldman, G., Gregg, W., Hooker, S., and Kuring, N.: Science quality SeaWiFS data for global biosphere research, Sea Technol., 39(9), 10–16, 1998.
Michaels, A. F. and Knap, A. H.: Overview of the US JGOFS Bermuda Atlantic Time-series study and the Hydrostation S program, Deep-Sea Res. Pt. II, 43(2–3), 157–198, doi:16/0967-0645(96)00004-5, 1996.
Mignot, A., Claustre, H., D'Ortenzio, F., Xing, X., Poteau, A., and Ras, J.: From the shape of the vertical profile of in vivo fluorescence to Chlorophyll-*a* concentration, Biogeosciences, 8, 2391–2406, doi:10.5194/bg-8-2391-2011, 2011.
Moore, T. S., Campbell, J. W., and Dowell, M. D.: A class-based approach to characterizing and mapping the uncertainty of the MODIS ocean chlorophyll product, Remote Sens. Environ., 113, 2424–2430, doi:10.1016/j.rse.2009.07.016, 2009.
Morel, A.: Optical modeling of the upper ocean in relation to its biogenous matter content (case-I waters), J. Geophy. Res.-Oceans, 93(C9), 10749–10768, 1988.
Morel, A. and Berthon, J.: Surface pigments, algal biomass profiles, and potential production of the euphotic layer-relationships reinvestigated in view of remote-sensing applications, Limnol. Oceanogr., 34(8), 1545–1562, 1989.
Morel, A. and Maritorena, S.: Bio-optical properties of oceanic waters: a reappraisal, J. Geophy. Res.-Oceans, 106(C4), 7163–7180, 2001.
Moutin, T. and Raimbault, P.: Primary production, carbon export and nutrients availability in Western and Eastern Mediterranean Sea in early summer 1996 (MINOS cruise), J. Marine Syst., 33–34(0), 273–288, doi:10.1016/S0924-7963(02)00062-3, 2002.

BGD
8, 11899–11939, 2011

Müller, P., Li, X.-P., and Niyogi, K. K.: Non-photochemical quenching, a response to excess light energy, Plant Physiol., 125(4), 1558–1566, doi:10.1104/pp.125.4.1558, 2001.
Ras, J., Claustre, H., and Uitz, J.: Spatial variability of phytoplankton pigment distributions in the Subtropical South Pacific Ocean: comparison between in situ and predicted data, Biogeosciences, 5, 353–369, doi:10.5194/bg-5-353-2008, 2008.
Rochford, P., Kara, A., Wallcraft, A., and Arnone, R.: Importance of solar subsurface heating in ocean general circulation models, J. Geophy. Res.-Oceans, 106(C12), 30923–30938, 2001.
Sharples, J., Moore, C. M., Rippeth, T. P., Holligan, P. M., Hydes, D. J., Fisher, N. R., and Simpson, J. H.: Phytoplankton distribution and survival in the thermocline, Limnol. Oceanogr., 46(3), 486–496, 2001.
Steinberg, D., Carlson, C., Bates, N., Johnson, R., Michaels, A., and Knap, A.: Overview of the US JGOFS Bermuda Atlantic Time-series study (BATS): a decade-scale look at ocean biology and biogeochemistry, Deep-Sea Res. Pt. II, 48(8–9), 1405–1447, 2001.
Strass, V.: On the calibration of large-scale fluorometric chlorophyll measurements from towed undulating vehicles, Deep-Sea Res., 37(3), 525–540, doi:16/0198-0149(90)90023-O, 1990.
Strickland, J. D. H.: Production of organic matter in primary stages of the marine food chain, in: Chemical Oceanography, edited by: Riley, J. P. and Skirrow, G., Academic Press, London, 477–610, 1965.
Strickland, J. D. H.: Continuous measurement of in vivo chlorophyll; a precautionary note, Deep-Sea Res., 15(2), 225–227, 1968.
Uitz, J., Claustre, H., Morel, A., and Hooker, S.: Vertical distribution of phytoplankton communities in open ocean: an assessment based on surface chlorophyll, J. Geophy. Res.-Oceans, 111(C8), C08005, doi:10.1029/2005JC003207, 2006.
Xing, X., Morel, A., Claustre, H., Antoine, D., D'Ortenzio, F., Poteau, A., and Mignot, A.: Combined processing and mutual interpretation of radiometry and fluorimetry from autonomous profiling bio-argo floats: Chlorophyll-*a* retrieval, J. Geophys. Res., 116, C06020, doi:10.1029/2010JC006899, 2011a.
Xing, X., Claustre, H., Blain, S., D'Ortenzio, F., Antoine, D., Ras, J., and Guinet, C.: Quenching correction for in vivo chlorophyll fluorescence measured by instrumented elephant seals in the Kerguelen region (Southern Ocean), Limnol. Oceanogr.-Meth., submitted, 2011b.

BGD
8, 11899–11939, 2011

Table 1. Sensitivity study on the impact of the resolution of the satellite extraction window of "HPLC" match-up. The percentage of valid match-ups, the median percent difference (MPD) between satellite and in-situ data as well as the determination coefficient (r^2) of the regression performed between two data sets are reported.

Temporal resolution	Spatial resolution	Percentage of valid match-ups	MPD	r^2
8 days	±0.25°	80.5 %	32 %	0.62
8 days	±0.1°	77.5 %	34 %	0.63
1 day	±0.25°	18.5 %	36 %	0.43

BGD
8, 11899–11939, 2011

Table 2. Quantity of fluorescence profiles available after each step of the data processing.

	DYFAMED	BATS	HOT
Raw data downloaded	184	2411	1912
Satellite Matchup	100	2145	1683
Quality Control	93	2049	1662
HPLC Matchup	55	109	104

BGD
8, 11899–11939, 2011

Table 3. Values of coefficients A and B, which relate the near surface [Chl-*a*] ($[\text{chl}]_{\text{surf}}$) to the integrated Chl-*a* content over Z_e ($\langle\text{chl}\rangle_{1Z_e}$) or $1.5Z_e$ ($\langle\text{chl}\rangle_{1.5Z_e}$). Values are directly reported from Uitz et al. (2006).

	well mixed waters	stratified waters	
		$[\text{chl}]_{\text{surf}} \leq 1\,\text{mg}\,\text{m}^{-3}$	$[\text{chl}]_{\text{surf}} > 1\,\text{mg}\,\text{m}^{-3}$
$\langle\text{chl}\rangle_{1Z_e} = A.[\text{chl}]^B_{\text{surf}}$	$A = 42.1$ m $B = 0.538$	$A = 36.1$ m $B = 0.357$	$A = 37.7$ m $B = 0.248$
$\langle\text{chl}\rangle_{1.5Z_e} = A.[\text{chl}]^B_{\text{surf}}$	$A = 58.5$ m $B = 0.546$	$A = 42.0$ m $B = 0.248$	$A = 43.5$ m $B = 0.847$

BGD
8, 11899–11939, 2011

Table 4. Comparison of "satellite-corrected" [Chl-*a*] with concomitant HPLC values.
The median "satellite-corrected" to HPLC [Chl-*a*] ratio, the semi-interquartile range (SIQR) measured on the previous series of ratio, the median percent difference (MPD) between "satellite-corrected" and HPLC data, as well as determination coefficient (r^2) of the regression performed between "satellite-corrected" and HPLC data points are reported. *N* indicates the number of couples of data points available. * refers to the variables which were calculated on log-transformed data.

	Median ratio*	SIQR*	MPD (%)	r^{2}*	*N*
total	1.01	0.16	30.9	0.67	2667
DYFAMED	0.94	0.29	40.9	0.70	500
BATS	1.00	0.15	30.3	0.62	1030
HOT	1.02	0.15	28.5	0.65	1137

BGD
8, 11899–11939, 2011

Table 5. Impact of the satellite [Chl-*a*] accuracy on the error of final calibrated profiles. The satellite error was measured with the relative percent difference (rpd) between satellite extracted [Chl-*a*] and near surface [Chl-*a*] derived from HPLC profiles. The accuracy of the merging method was assessed with the median absolute percent difference (MPD) between "satellite-corrected" and HPLC data points.

Satellite error	rpd < −30		−30 < rpd < 30		rpd > 30		Total
	MPD	*N*	MPD	*N*	MPD	*N*	MPD
DYFAMED	53.5	36	35.4	145	40.5	319	40.9
BATS	28.4	120	25.2	428	36.0	482	30.3
HOT	27.4	159	28.8	703	28.1	275	28.4

BGD
8, 11899–11939, 2011

Table 6. Comparison, on a subset of DYFAMED data, of "satellite-corrected" and "Boss-calibrated" [Chl-*a*] with concomitant HPLC values.
See the caption of Table 4 for details about parameters.

	Median ratio*	SIQR*	MPD (%)	r^{2}*	*N*
Boss et al. (2008)	0.98	0.24	42.7	0.87	224
Present paper	0.92	0.27	43.5	0.77	224

BGD
8, 11899–11939, 2011

Table 7. Comparison between "satellite-corrected" [Chl-*a*] and concomitant HPLC values after having applied a monthly average filter.
See the caption of Table 4 for details about parameters.

	Median ratio*	SIQR*	MPD (%)	r^{2}*	*N*
total	1.01	0.11	21.2	0.82	432
DYFAMED	1.03	0.30	33.4	0.80	144
BATS	1.01	0.08	17.0	0.86	144
HOT	1.00	0.10	17.1	0.81	144

BGD
8, 11899–11939, 2011

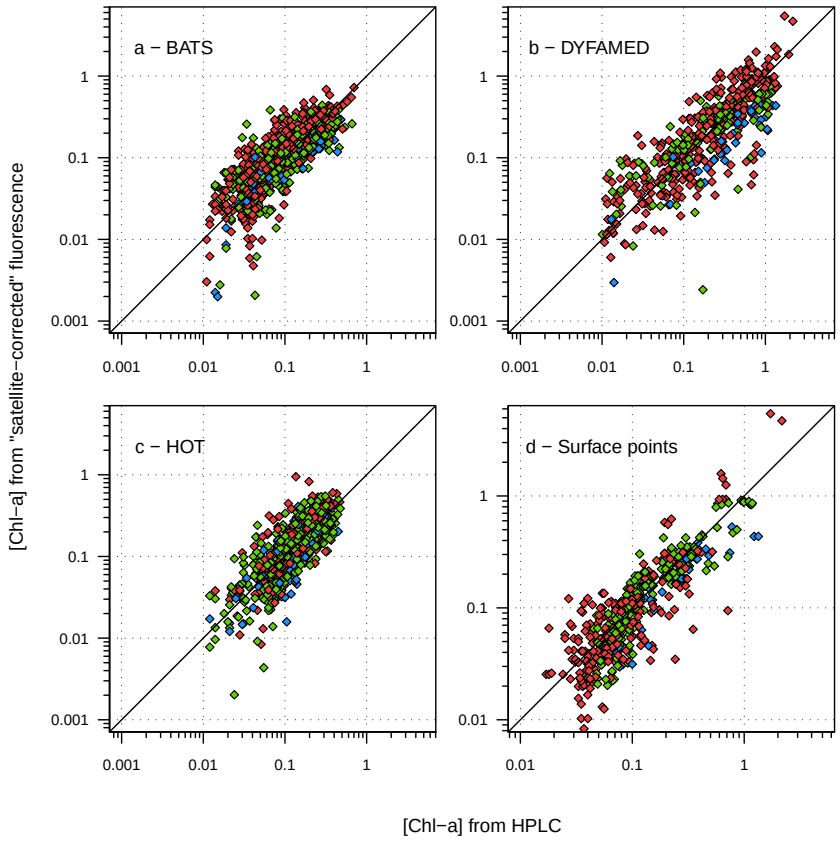

Fig. 1. Scatter plots of "satellite-corrected" [Chl-*a*] as a function of concomitant HPLC [Chl-*a*], in mg m^{-3}. Colours characterize the error of satellite in the estimation of near surface [Chl-*a*]: overestimation exceeding 30 % (red), underestimation exceeding 30 % (blue) and error inferior to ± 30 % (green). Only surface points, above 20 m depth, are displayed in panel **(d)**.

BGD
8, 11899–11939, 2011

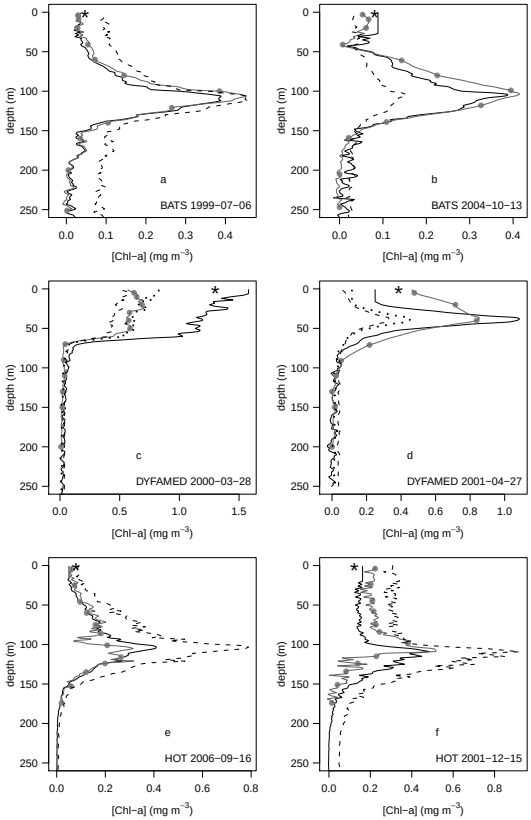

Fig. 2. Examples of "satellite-corrected" profiles (black solid line), "HPLC calibrated" profiles (grey solid line), factory calibrated fluorescence profiles (black dashed line) and, only for DYFAMED examples, "Boss-calibrated" profiles (black dotted lines). In complement, HPLC data points are indicated by grey circles and satellite surface [Chl-*a*] by black stars.

BGD
8, 11899–11939, 2011

Towards a merged satellite and in situ fluorescence ocean chlorophyll product

H. Lavigne et al.

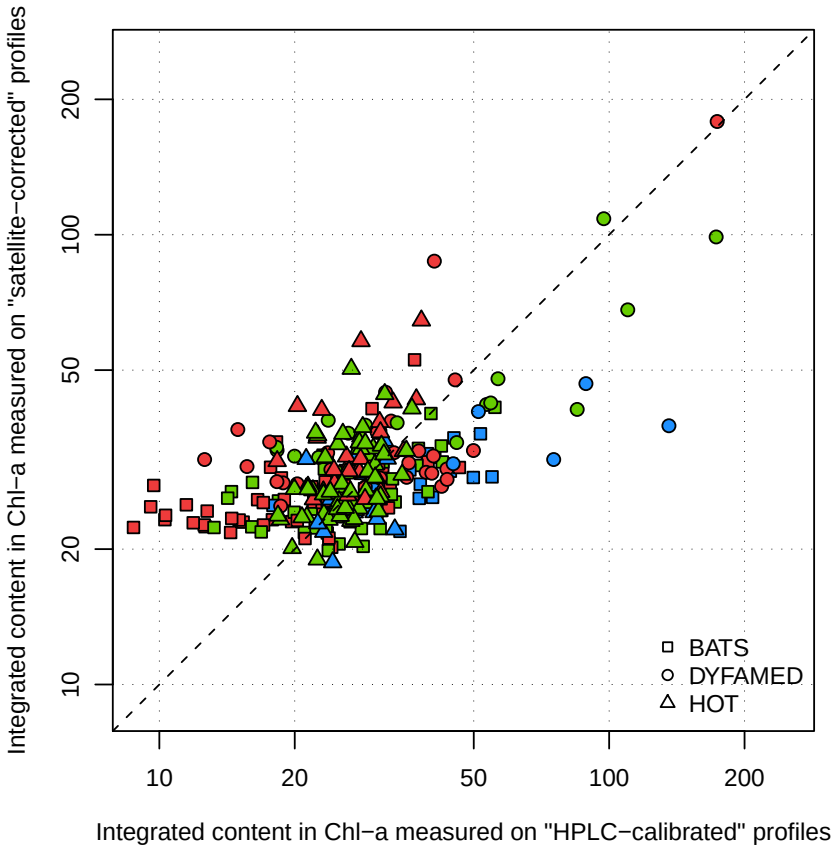

Fig. 3. Scatter plot of integrated Chl-*a* content over 200 m computed on "satellite-corrected" profiles, as a function of integrated Chl-*a* content computed on "HPLC-calibrated" profiles. Both Chl-*a* contents are expressed in mg m^{-2}. Similarly to Fig. 1, colour code refers to the error of satellite in the estimation of near-surface [Chl-*a*].

BGD
8, 11899–11939, 2011

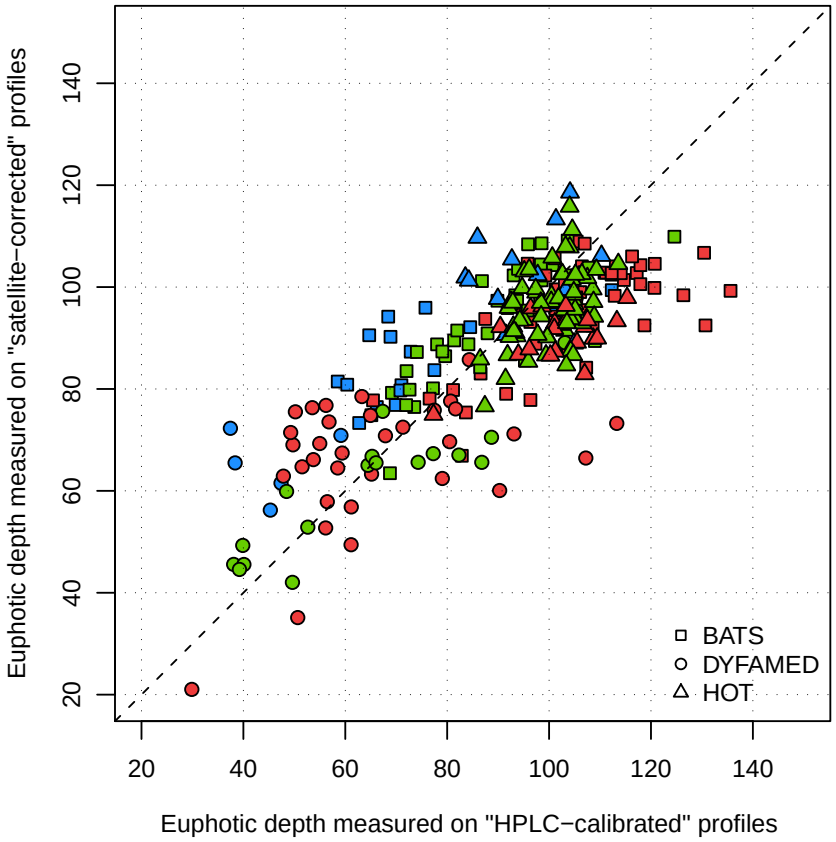

Fig. 4. Scatter plot of the euphotic depth computed on “satellite-corrected” profiles as a function of the euphotic depth computed on “HPLC-calibrated” profiles using the algorithm described by Morel and Berthon (1989). Both euphotic depths are expressed in m. Similarly to Fig. 1, colour code refers to the error of satellite in the estimation of near-surface [Chl-*a*].

BGD
8, 11899–11939, 2011

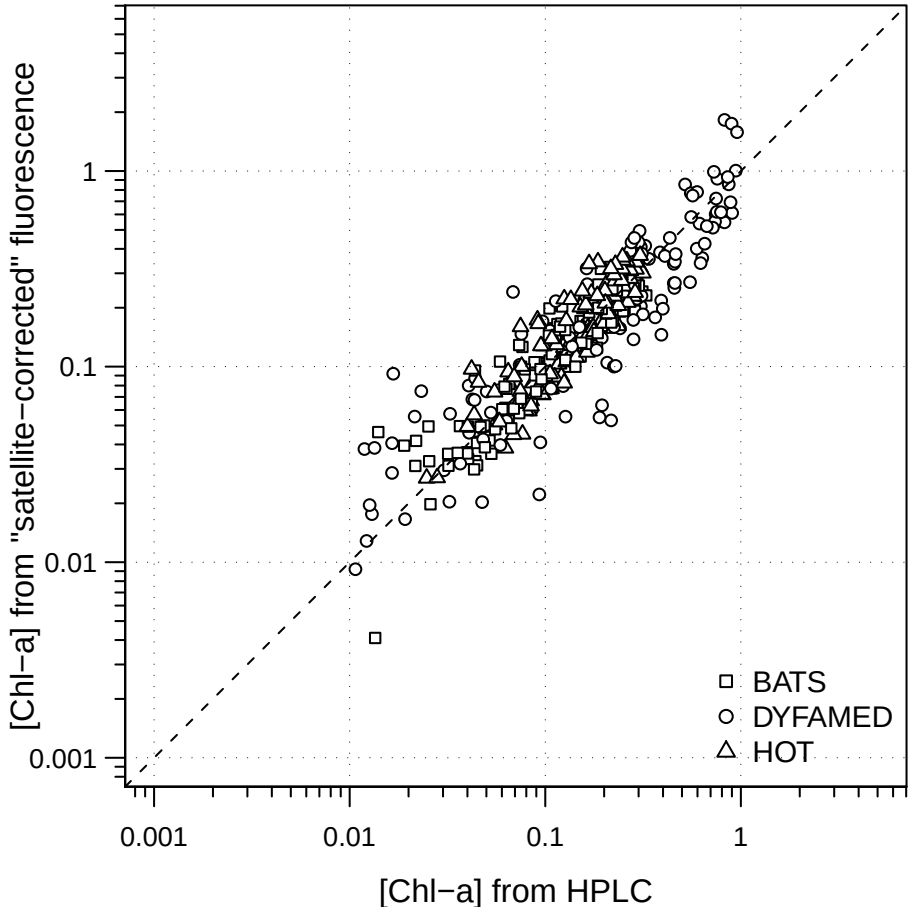

Fig. 5. Scatter plot of [Chl-*a*] derived from "satellite-corrected" fluorescence profiles as a function of [Chl-*a*] measured with HPLC, after having applied a monthly average filter. [Chl-*a*] is expressed in mg m^{-3}.

BGD
8, 11899–11939, 2011

Towards a merged satellite and in situ fluorescence ocean chlorophyll product

H. Lavigne et al.

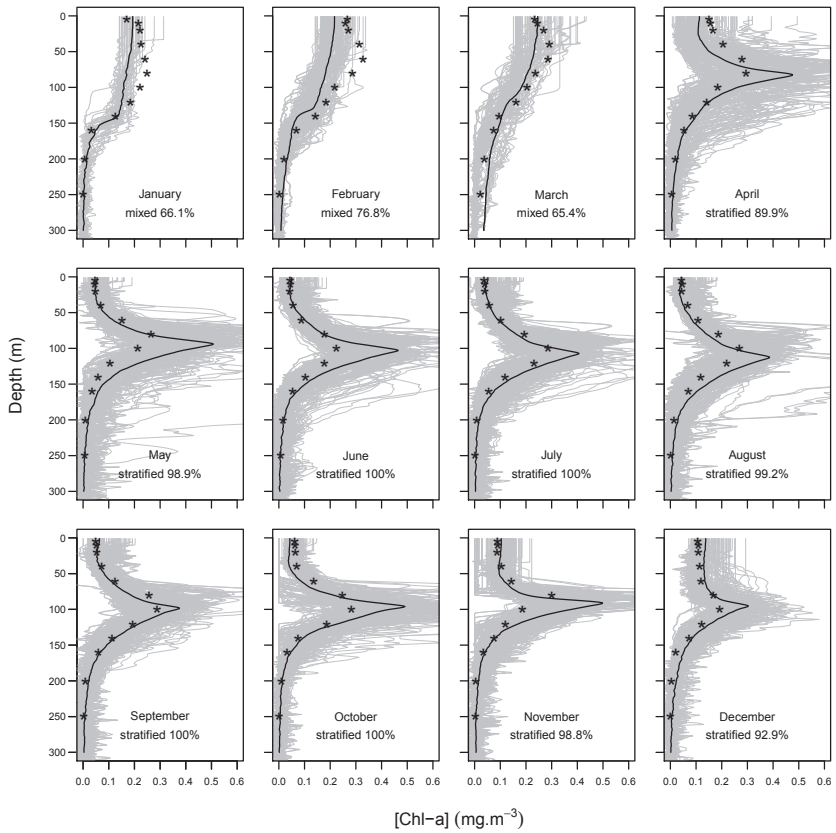

Fig. 6. Comparison of the BATS monthly fluorescence-based [Chl-*a*] climatology (black solid lines) to the HPLC-based climatology (black stars, see text and Appendix A for details about computation methods). For the fluorescence-based climatology, the retained shape (i.e. "stratified" or "mixed") is indicated with its percentage of occurrence and grey lines display all the "satellite-corrected" profiles representing the dominant shape.

BGD
8, 11899–11939, 2011

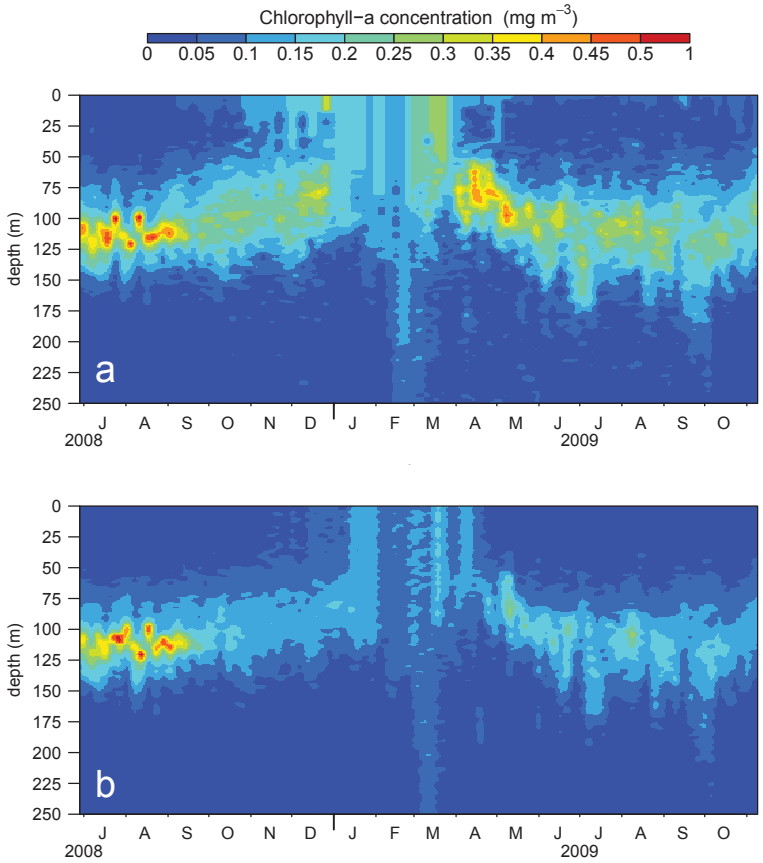

Fig. 7. Time-series of [Chl-*a*] distribution estimated with a fluorometer deployed on a profiling float in the Levantine Sea, and processed with the present method (panel **a**) and with the Boss et al. (2008) method (panel **b**).

BGD
8, 11899–11939, 2011